The Plant Cell, Vol. 10, 1927–1939, November 1998, www.plantcell.org © 1998 American Society of Plant Physiologists

A *GFP–MAP4* Reporter Gene for Visualizing Cortical Microtubule Rearrangements in Living Epidermal Cells

Jan Marc,[a] Cheryl L. Granger,[b] Jennifer Brincat,[b] Deborah D. Fisher,[b] Teh-hui Kao,[c] Andrew G. McCubbin,[c] and Richard J. Cyr[b,1]

[a] Biological Sciences, University of Sydney, Sydney 2006, Australia
[b] Department of Biology, Pennsylvania State University, University Park, Pennsylvania 16802-5301
[c] Department of Biochemistry and Molecular Biology, Pennsylvania State University, University Park, Pennsylvania 16802-5301

Microtubules influence morphogenesis by forming distinct geometrical arrays in the cell cortex, which in turn affect the deposition of cellulose microfibrils. Although many chemical and physical factors affect microtubule orientation, it is unclear how cortical microtubules in elongating cells maintain their ordered transverse arrays and how they reorganize into new geometries. To visualize these reorientations in living cells, we constructed a microtubule reporter gene by fusing the microtubule binding domain of the mammalian microtubule-associated protein 4 (*MAP4*) gene with the green fluorescent protein (*GFP*) gene, and transient expression of the recombinant protein in epidermal cells of fava bean was induced. The reporter protein decorates microtubules in vivo and binds to microtubules in vitro. Confocal microscopy and time-course analysis of labeled cortical arrays along the outer epidermal wall revealed the lengthening, shortening, and movement of microtubules; localized microtubule reorientations; and global microtubule reorganizations. The global microtubule orientation in some cells fluctuates about the transverse axis and may be a result of a cyclic self-correcting mechanism to maintain a net transverse orientation during cellular elongation.

INTRODUCTION

Microtubules are arranged in different arrays, which perform a variety of essential functions within the cell (Lloyd, 1991). During interphase, microtubules are organized predominately into a cortical array, where they are involved in directing cellulose deposition, which consequently plays a fundamental role in cellular morphogenesis (Giddings and Staehelin, 1991; Cyr, 1994). Individual cortical microtubules are up to 10 μm long and are arranged parallel to one another with overlapping ends (Williamson, 1991; Vesk et al., 1994). They may be cross-bridged with other microtubules and/or linked to the plasma membrane or to other cytoskeletal components, and they may assemble into strands that are continuous from one cell face to another (Flanders et al., 1989; Yuan et al., 1995). Within the cells of elongating tissues, microtubules generally form cylindrical arrays in which their strands are oriented transversely or at slightly oblique angles to the direction of cell elongation (reviewed in Green, 1980; Gunning and Hardham, 1982; Cyr and Palevitz, 1995; Wymer and Lloyd, 1996; Fischer and Schopfer, 1997). At the completion of the elongation phase, microtubules usually reorient into a more oblique or even longitudinal direction. Unique arrays operate during the differentiation of specialized cells, such as the banded patterns in tracheary elements (Fukuda, 1997) or radial arrays in stomatal guard cells (Marc et al., 1989). The cortical array's significance in morphogenesis has been documented by studies with antimicrotubule drugs, which depolymerize microtubules and cause cells to grow isodiametrically (Morejohn, 1991), and by the mutants *ton* and *fass* of Arabidopsis, which have aberrant cortical microtubules and possess abnormally shaped cells (Traas et al., 1995; McClinton and Sung, 1997).

The spatial orientation of microtubules in the cortex is complex and likely involves interactions with a variety of auxiliary molecules and complexes. For example, microtubule-organizing centers nucleate microtubules and thereby affect their appearance in the cortex (reviewed in Marc, 1997; Vaughn and Harper, 1998), whereas microtubule-associated proteins (MAPs) may serve to link microtubules to each other and to other organelles (reviewed in Cyr, 1991; Hirokawa, 1994; Mandelkow and Mandelkow, 1995) and also to modify microtubule stability, thereby affecting their organization and dynamics (Hirokawa, 1994; Desai and Mitchison, 1997). Phosphorylation of MAPs may play a role in organization because this post-translational modification alters their affinity for microtubules, thereby causing rearrangements of the microtubular network (Preuss et al., 1995; Hush et al., 1996; Shelden and Wadsworth, 1996); moreover, treatments with inhibitors of protein phosphatases and kinases disorganize cortical microtubules (Mizuno, 1994; Baskin and Wilson,

[1] To whom correspondence should be addressed. E-mail rjc8@psu.edu; fax 814-865-9131.

1997). Mechanochemical motor proteins could affect microtubule organization by facilitating the translocation of elements within the array (Asada and Shibaoka, 1994; Cyr and Palevitz, 1995; Wymer et al., 1996a). In addition, actin microfilaments appear to regulate microtubule organization in differentiating tracheary elements (Fukuda, 1997). The organization of the microtubules likely involves noncytoskeletal components because recent work with inhibitors of cellulose synthesis shows that the organization of cortical microtubules into an ordered array requires the presence of the cell wall, indicating that the flow of information between the cytoskeleton and the cell wall is bidirectional (Fisher and Cyr, 1998) and may be coordinated across the tissue (Liang et al., 1996).

Our understanding of the organizing mechanism is further complicated by chemical and physical factors that modify microtubule orientation while inducing corresponding changes in the growth rate of cells. Among plant growth substances, auxins, gibberellins, and brassinolide generally promote cell elongation and transverse alignment of microtubules. Ethylene, abscisic acid, and cytokinins induce oblique or longitudinal microtubule orientation and decrease growth rates (reviewed in Shibaoka, 1994; Fischer and Schopfer, 1997). Microtubule orientation can also be influenced by physical factors, such as light (Iwata and Hogetsu, 1989; Zandomeni and Schopfer, 1993), gravity (Blancaflor and Hasenstein, 1995), and centrifugation (Wymer et al., 1996b), and by biophysical forces, such as mechanical extension and compression (Zandomeni and Schopfer, 1994). Interestingly, mechanical forces can modulate the effects of auxin and light (Fischer and Schopfer, 1997), suggesting that there are synergistic effects among the various modulating factors.

Microtubule organization is a dynamic process. Whereas the traditional methods for visualizing microtubules in fixed cells by electron microscopy and immunofluorescence microscopy have revealed a wealth of information, studies with living cells have extended our knowledge even further (reviewed in Hepler and Hush, 1996; Wymer and Lloyd, 1996). For example, microinjected tubulin rapidly incorporates until the number and length of microtubules reach a steady state, after which the labeled microtubules remain visible for several hours (Wasteneys et al., 1993; Yuan et al., 1994). In elongating cells of *Nitella* and stamen hairs of *Tradescantia*, some microtubules remain stable, whereas others change in length or location within minutes, although a predominantly transverse orientation is maintained even during recovery after depolymerization with oryzalin (Wasteneys et al., 1993; Kropf et al., 1997). In contrast, microinjection of pea epidermal cells induces a rapid (~1 hr) reorientation of initially transverse microtubules along the outer epidermal wall into a longitudinal alignment (Yuan et al., 1994, 1995).

The technique of microinjecting fluorescent tubulin analogs has its limitations. Besides being tedious, the operation may perturb the cells, the addition of exogenous tubulin may elevate the cytoplasmic pool of assembly-competent tubulin, stable microtubules may go undetected, and the observation times are limited (Stearns, 1995; Wymer and Lloyd, 1996). An advanced technology, which circumvents some of these problems, uses genetic transformation with a reporter gene that encodes the green fluorescent protein (GFP) from the jellyfish *Aequorea victoria* (Chalfie et al., 1994; Ludin and Matus, 1998). A number of genetic modifications of the molecule have produced versions of the protein with improved spectral properties and stability (Cubitt et al., 1995; Heim and Tsien, 1996; Rizzuto et al., 1996). Additional modifications to optimize the codon usage for proper mRNA processing in plants (Haseloff and Amos, 1995; Sheen et al., 1995) have further increased the utility of this reporter. In plants, GFP has been used successfully to track viral movement proteins (Heinlein et al., 1995; Epel et al., 1996; Oparka et al., 1996; Blackman et al., 1998), to localize phragmoplastin (Gu and Verma, 1997), and to study *Rhizobium* Nod factors (van de Sande et al., 1996). In addition, GFP has been used to localize cytoskeletal elements, including yeast tubulin, neuronal MAP2C, Tau34, *Dictyostelium* actin, and yeast myosin (reviewed in Ludin and Matus, 1998).

A chimeric gene containing both *GFP* and a modified mammalian *MAP4* sequence has been used successfully to label microtubules in mammalian cells (Olson et al., 1995). Because tubulins are highly conserved, we reasoned that inserting a similar construct into a plant expression vector and then transforming plant cells with the recombinant DNA would generate a fusion protein that would bind to plant microtubules. Herein, we present data showing that the fusion protein binds to microtubules in vivo and is useful for a range of studies within the living cells of higher plants.

RESULTS

Construction of the Microtubule Reporter Gene *GFP–MBD*

The binding properties of the microtubule binding domain (MBD) of the mammalian MAP4 and its effects on microtubule dynamics and stability, as well as the utility of GFP–MBD fusion protein constructs for localizing microtubules, have been analyzed in mammalian cells (Olson et al., 1995). The MBD contains a proline-rich region (P) and a region that is abundant in serine and proline (SP) that together bind strongly to microtubules and induce their bundling. The remainder of the domain is occupied by degenerate repeats (PGGG) that enhance microtubule binding, probably by stabilizing assembled tubulin heterodimers (West et al., 1991; Olson et al., 1995). Because MAP binding sites on the tubulin molecule appear to be conserved between plants and animals (Hugdahl et al., 1993), we reasoned that the MBD would also bind to plant microtubules in vivo.

To test the hypothesis that MAP binding sites are conserved between plants and animals and to develop a useful microtubule reporter gene, we constructed a *GFP–MBD* chi-

meric gene compatible for use in plants. This construct was created by fusing a plant-optimized GFP cDNA (Chiu et al., 1996) upstream of the MBD cDNA and inserting the resulting recombinant gene between the cauliflower mosaic virus 35S promoter and the nopaline synthase terminator of the pUC18 plasmid vector. The authenticity of the construct was confirmed by sequencing. The arrangement of individual components of the reporter gene is shown in Figure 1.

Binding Specificity of the Reporter Protein

We introduced the GFP–MBD construct into the epidermis on the lower side of fava bean leaves by biolistic particle bombardment (Christou, 1996). When the leaves were examined with an epifluorescence microscope equipped with a fluorescein isothiocyanate filter set, a fluorescent signal appeared as distinct filaments without a noticeable diffuse signal in the cytoplasm, indicating that the reporter protein has a high binding affinity for the filaments.

The location and orientation of filamentous images observed by using this method are consistent with the location of microtubules previously demonstrated by other techniques (Williamson, 1991; Cyr and Palevitz, 1995). Figure 2A depicts a cell with the characteristic fluorescing filaments. To verify the microtubule nature of these filaments, fluorescent cells were located and recorded within leaves 4 hr after bombardment (Figure 2A). The leaves were then placed in the antimicrotubule herbicide amiprophosmethyl (20 μM), and the fluorescing cells were reexamined. Periodic observation of these cells revealed that the filaments were sensitive to the drug and that they started to break down within 30 min of incubation (Figure 2B). The filaments progressively disintegrated, with concurrent formation of small cytoplasmic pools, until they disappeared (Figures 2C and 2D). Similar results were obtained with oryzalin and colchicine or by incubating the leaves on ice (data not shown). Leaves that were incubated only with water had distinct filaments that maintained their integrity for many hours.

As an additional confirmation for microtubule binding, we used an in vitro microtubule cosedimentation assay to examine the interaction between the chimeric gene product and microtubules. We fused the *GFP–MBD* sequence downstream of the glutathione *S*-transferase (*GST*) gene of the pGEX-2T vector. The *GST–GFP–MBD* chimeric gene was expressed in *Escherichia coli* and was found to fluoresce with an excitation maximum at 490 nm and emission maximum at 510 nm, which correspond to the published values for this GFP derivative (S65T; Heim and Tsien, 1996). Electrophoresis of the total solubilized proteins by using SDS-PAGE revealed a major fluorescing band with an M_r of 103,000, as seen in Figure 3, lane 1, which is similar to the predicted molecular mass of 97 kD of the GST–GFP–MBD fusion protein. Minor bands of lower molecular weight are probably proteolytic fragments. When taxol-stabilized microtubules were added, followed by centrifugation, the fluorescent protein disappeared from the supernatant (Figure 3, lane 2) and reappeared in the pellet (Figure 3, lane 3). This

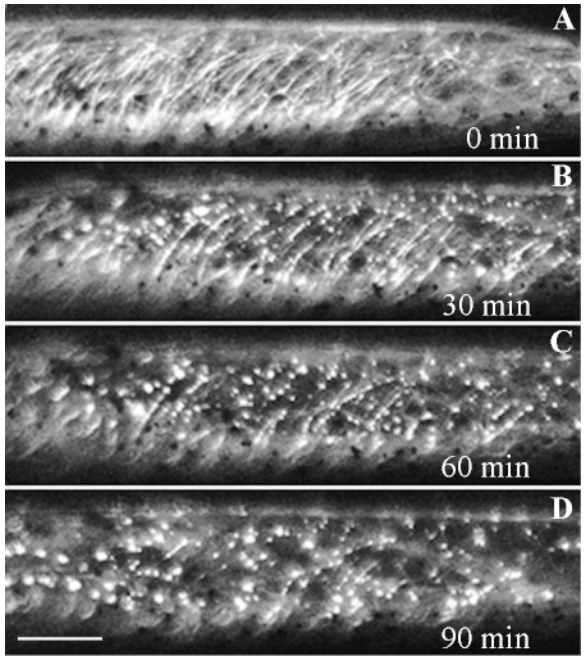

Figure 2. Laser Scanning Confocal Microscopic Images of a Transformed Epidermal Cell from a Fava Bean Leaf Vein during Incubation with the Antimicrotubule Drug Amiprophosmethyl (APM).

The lower side of a fava bean leaf was bombarded with the *GFP–MBD* reporter gene; 4 hr later, the leaf was incubated with 20 μM APM.
(A) Before the addition of APM.
(B) 30 min after the addition of APM.
(C) 60 min after the addition of APM.
(D) 90 min after the addition of APM.
All images represent the cortical region along the outer epidermal wall of the same cell. The images show progressive disintegration of microtubules into small cytoplasmic pools. Bar in **(D)** = 20 μm for **(A)** to **(D)**.

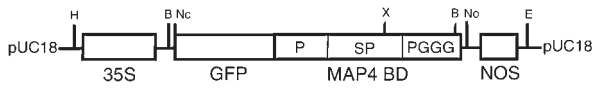

Figure 1. Schematic Diagram of the *GFP–MBD* Chimeric Gene.

MBD of MAP4 (MAP4 BD) includes proline-rich (P), serine/proline–rich (SP), and degenerate repeat (PGGG) subdomains. The junction between *GFP* and MBD is at *GFP* nucleotide position 744 and *MAP4* nucleotide position 2408. Vertical bars indicate the positions of restriction sites used in cloning. The construct, flanked by the 35S promoter (35S) and the nopaline synthase (NOS) terminator, was inserted into a pUC18 plasmid vector.

sedimentation was strictly dependent on the presence of microtubules, because no fluorescing band appeared in the pellet if microtubules were not added (Figure 3, lane 6). Furthermore, a construct made of GST–GFP alone (53 kD) showed no convincing evidence for microtubule-dependent sedimentation (Figure 3, lane 9). We conclude that the GFP–MBD recombinant protein binds to microtubules specifically via the MBD.

Characteristics of GFP–MBD Expression

The cortical microtubule arrays along the outer epidermal walls had various arrangements. Although random arrangements were observed in some cells, such as those seen in the cell depicted in Figure 4D, most cells had highly ordered arrays. We categorized these orientations into transverse (60 to 90° to the long axis of the cell; Figure 4A), oblique (30 to 60°; Figure 4B), or longitudinal (0 to 30°; Figure 4C). Some cells had regional differences in microtubule orientation or even microtubules of mixed orientations in the same region. After extended periods of expression (>10 hr), some cells contained relatively fewer but thicker and longer microtubule cables throughout the cytoplasm, as shown in Figure 5A. A few cells contained highly fluorescent elongate aggregates (Figure 5B), which occasionally drifted around the cytoplasm (data not shown).

Fluorescent signals appeared 2 to 3 hr after bombardment and persisted for 1 to 2 days. Generally, the intensity of the fluorescent signal, which presumably corresponds to the level of gene expression, varied among different cells and differed even between some neighboring cells. In many cells, signal intensity increased markedly over several hours. This presumably reflects increased protein expression, increased microtubule bundling, or addition of newly deco-

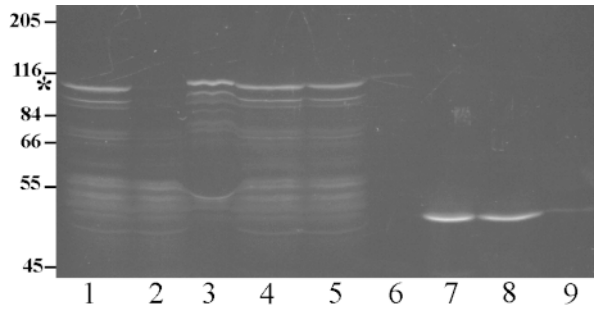

Figure 3. Cosedimentation of Bacterial Recombinant GFP–MBD Protein with Taxol-Stabilized Microtubules.

The GST–GFP–MBD and GST–GFP fusion proteins were expressed in *E. coli*, and total soluble proteins were extracted for microtubule binding experiments. Taxol was added at a final concentration of 10 μM, and the samples were prespun at 55,000*g* for 10 min. Taxol-stabililized microtubules, or buffer, were added to the samples for 45 min, and the samples were then centrifuged as before, with the pellet and supernatants being separated and subjected to SDS-PAGE. The gel was placed on a UV light box and photographed using a 500- to 520-nm bandpass filter. Lane 1 contains total bacterial protein with GST–GFP–MBD before the addition of microtubules; lane 2, supernatant after microtubule sedimentation; lane 3, microtubule pellet with cosedimented proteins; lane 4, total bacterial protein with GST–GFP–MBD before the addition of buffer; lane 5, supernatant after sedimentation; lane 6, pellet after buffer sedimentation; lane 7, total bacterial protein with GST–GFP before the addition of microtubules; lane 8, supernatant after microtubule sedimentation; and lane 9, microtubule pellet with cosedimented proteins. The position of the GST–GFP–MBD polypeptide is indicated by an asterisk. Labels at left indicate the positions of molecular mass standards in kilodaltons.

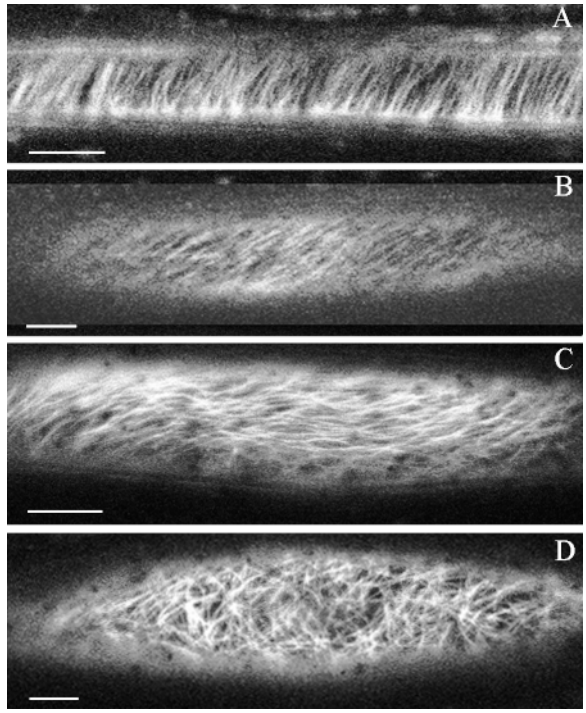

Figure 4. Representative Laser Scanning Confocal Microscopic Images of Cortical Microtubule Arrays along the Outer Epidermal Wall in Different Cells.

Fava bean leaves were bombarded on their lower side with the *GFP–MBD* construct and then maintained in a humid Petri dish. The whole leaf was examined periodically with a laser scanning confocal microscope for several hours after bombardment.
(A) Ordered array with almost transverse orientation 21 hr after bombardment.
(B) Ordered array at oblique angle 25 hr after bombardment.
(C) Ordered longitudinal array 5 hr after bombardment.
(D) Microtubules in random orientations 5 hr after bombardment.
Bars in **(A)** to **(D)** = 20 μm.

rated microtubules to the existing bundles. As shown in Figure 6, the expression became detectable ~3 hr after bombardment and, in this cell, revealed a wavy longitudinal array (Figure 6A). In this cell, the spatial organization of the array remained stable while the signal intensity increased dramatically during the following 3 hr (Figures 6B and 6C). After 10 hr, the array became converted into long microtubule cables located in the cortex as well as deeper in the cytoplasm (Figure 6D).

GFP–MBD Reveals Microtubule Dynamics

Dynamic changes were often observed in cells expressing relatively low amounts of the GFP–MBD protein, and spatial alterations over time were noted in microtubules, in groups of microtubules within localized regions, and globally along the outer epidermal wall. Figure 7 shows the dynamics of a microtubule: a new microtubule appeared in a free area within 10 min of observation (Figures 7A and 7B), it elongated and reoriented somewhat over the next 20 min (Figure 7C), and almost disappeared again in the following 10 min (Figure 7D).

Regional rearrangements within a localized population of microtubules were also noted. In the cell shown in Figure 8A, there was initially a mixed orientation of microtubules to the left of center (arrows). Over time, these discordant microtubules became globally aligned with other microtubules throughout the outer face of the array. A similar localized reorganization was seen in the cell depicted in Figure 9A.

Global reorientations of cortical microtubules occurred along the entire outer epidermal wall and were most notable in dimly fluorescent cells expressing low levels of the GFP–MBD protein. In the example shown in Figure 8, most of the microtubules were initially transverse or oblique and oriented to the right at 21 hr after bombardment (Figure 8A). The array became more transverse 4 hr later (Figure 8B) and then gradually reoriented to oblique angles oriented to the left during the next 6 hr (Figures 8C and 8D). Figures 9A to 9D show a cell in which most of the microtubules were initially

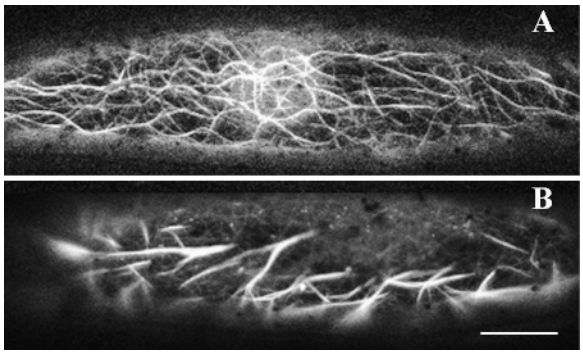

Figure 5. Laser Scanning Confocal Microscopic Images of Cortical Microtubule Arrays Expressing High Levels of the Recombinant Protein.

Fava bean leaves were bombarded and then maintained in a humid Petri dish before being examined with a laser scanning confocal microscope.
(A) Thick and long microtubule bundles 22 hr after bombardment.
(B) Crystalline microtubule aggregates 22 hr after bombardment.
Bar in **(B)** = 30 μm for **(A)** and **(B)**.

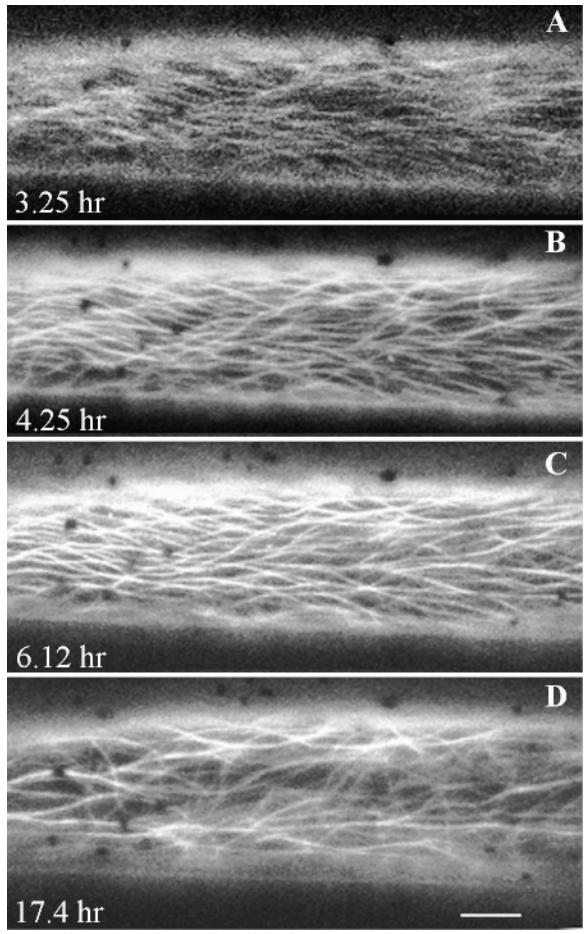

Figure 6. A Time Sequence of Laser Scanning Confocal Microscopic Images of a Microtubule Array within a Cell's Cortex along the Outer Epidermal Wall.

A fava bean leaf was bombarded and maintained in a humid Petri dish for 21 hr and then viewed with a laser scanning confocal microscope at various times.
(A) 3.2 hr after bombardment.
(B) 4.2 hr after bombardment.
(C) 6.1 hr after bombardment.
(D) 17.4 hr after bombardment.
The signal intensity increased markedly during the first 6 hr and was followed by the formation of long cables. Bar in **(D)** = 10 μm for **(A)** to **(D)**.

transverse. Over the next 10 hr, the array became more oblique and then began to reorient back toward the initial position. In many cases, these rearrangements occurred throughout the length of the outer epidermal wall, although some were confined to a limited region of the wall (data not shown). Typically, the alternating changes in pitch were most apparent in cells with fine and dim cortical arrays rather than in cells with prominent microtubule bundles.

DISCUSSION

Binding Specificity of the Microtubule Reporter Protein

MAPs bind to microtubules via the highly charged C termini on tubulin (Nogales et al., 1998). This region is present in all eukaryotic tubulin genes, suggesting that the MAP binding sites are also conserved (Burns and Surridge, 1994). Because of this conservation, we reasoned that a mammalian microtubule binding domain would bind plant microtubules; thus, we designed a GFP mammalian binding domain reporter protein, GFP–MBD, for labeling plant microtubules.

For GFP–MBD to act as a successful reporter protein, the fusion of MBD with GFP should not change the microtubule binding function of the MBD. The molecular mass of GFP is 29 kD (Ormo et al., 1996) and the calculated mass of the MBD is ~40 kD, resulting in a total mass of ~70 kD. Based on size, the 70-kD chimeric protein should not interfere with the function of the 100-kD α/β-tubulin heterodimer to any greater extent than would native plant MAPs, which can range in size upward to 125 kD (Durso and Cyr, 1994; Cyr and Palevitz, 1995; Chan et al., 1996; Marc et al., 1996). The GFP–MBD construct retains its ability to bind microtubules, as evidenced by three criteria: first, the fluorescent filamentous pattern displayed is typical of the spatial arrangement of microtubules in the cell's cortex; second, a bacterially expressed recombinant protein binds to microtubules in vitro; third, the filamentous pattern is sensitive to antimicrotubule herbicides and to low temperatures.

The versatility of GFP–MBD in binding microtubules is demonstrated by the fact that we have visualized filamentous arrays not only in the leaf epidermis of fava bean but also in the leaf epidermis of other plant species, including Arabidopsis, tobacco, and onion. We have also seen arrays in stomatal guard cells and lobed epidermal cells along the lamina. The binding of this protein to microtubules within the cortical arrays of different plant species and within various cell types confirms the evolutionary conservation of the MAP binding sites on the tubulin molecule.

Characteristics of GFP–MBD Expression

Particle bombardment is an efficient method for introducing heterologous DNA into leaf epidermal cells, generating ~10 to 100 transformed cells per leaf. This technique results in very rapid protein expression (within 2 to 3 hr) that lasts 1 to 2 days. Bombarded cells appear viable, because normal cytoplasmic streaming continues, and the dimly fluorescent microtubules have patterns similar to those reported in other plant cells (Cyr and Palevitz, 1995). Transformed cells remain alive for at least 2 days, allowing extended time-course observations of microtubules and perfusion with drug solutions. Wounding does not appear to be problematic. Occasionally, necrosis occurred in the region of the leaf impacted

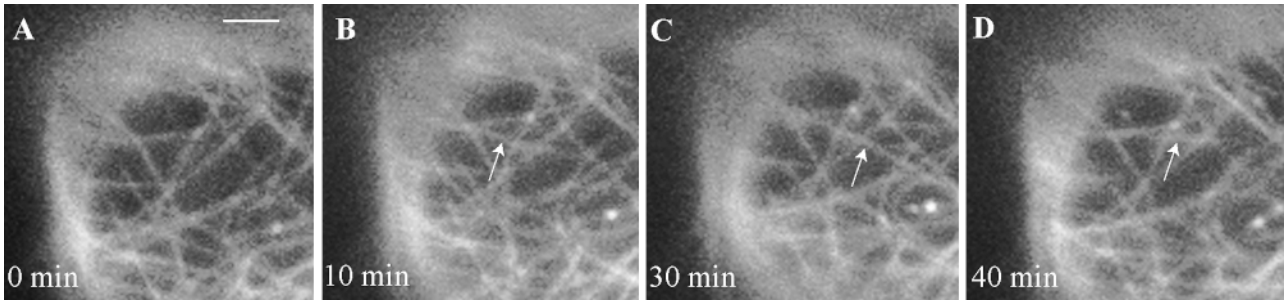

Figure 7. Laser Scanning Confocal Microscopic Images of a Cortical Microtubule Array near the Tip of an Epidermal Cell of a Fava Bean Leaf.

A fava bean leaf was bombarded and maintained in a humid Petri dish for 20 hr before examination using a laser scanning confocal microscope. Images were taken at consecutive intervals and show a microtubule array in the cortex near the tip of the cell along the outer epidermal wall. The arrows indicate the same microtubule at various observational times.

(A) 0 min.

(B) 10 min.

(C) 30 min.

(D) 40 min.

Bar in **(A)** = 5 μm for **(A)** to **(D)**.

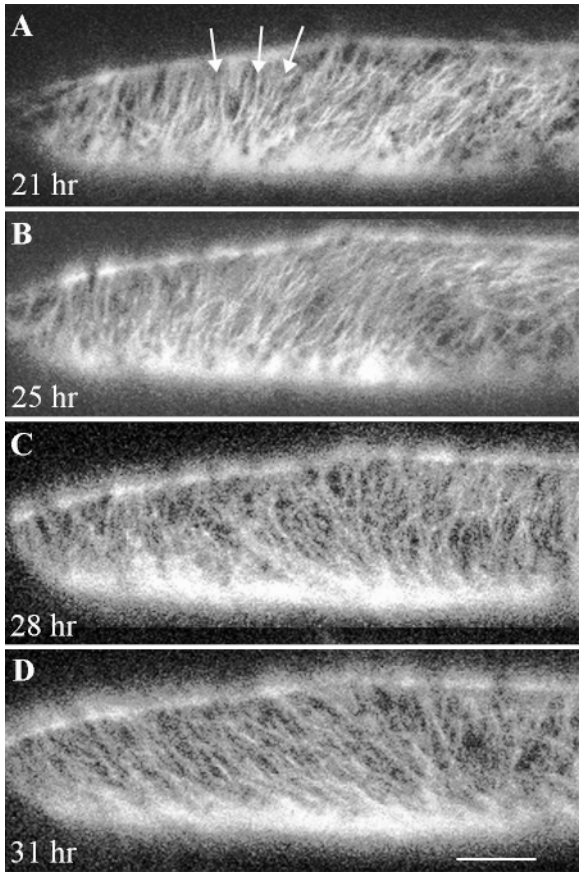

Figure 8. Time Sequence of Laser Scanning Confocal Microscopic Images of a Microtubule Array in the Cortex along the Outer Epidermal Wall of a Fava Bean Leaf Showing Net Movement in One Direction.

A fava bean leaf was bombarded and maintained in a humid Petri dish for 21 hr and then viewed with a laser scanning confocal microscope at various times.
(A) 21 hr after bombardment.
(B) 25 hr after bombardment.
(C) 28 hr after bombardment.
(D) 31 hr after bombardment.
Most of the microtubules in the array were initially transverse or oblique with a pitch to the right, but gradually they swayed to the left. The arrows in **(A)** point to some microtubules that appeared initially to have mixed orientations. Bar in **(D)** = 20 μm for **(A)** to **(D)**.

by the gold particles, but such samples were not included in our analyses.

Decoration with GFP–MBD produced a smooth, continuous outline of microtubules oriented in transverse, oblique, longitudinal, or random arrays. The resolution equals or surpasses that obtained with immunofluorescence microscopy. The fluorescent microtubule images have a high signal/noise ratio, indicating a high binding affinity of the expressed protein for microtubules rather than an accumulation in the cytoplasmic pool. The signal is remarkably stable, presumably as a result of the chromophore being protected inside the barrel-shaped GFP molecule (Ormo et al., 1996), allowing repeated observations without noticeable bleaching. There was no evidence of a phototoxic effect in cells that had been repeatedly imaged.

Most cells had microtubule images that were intermediate in intensity; however, variations in brightness and intensity did occur. These variations may reflect differences in expression of the transgene and/or differences in microtubule organization. The dimmer images may indicate the presence of single microtubules, whereas the brightest images may

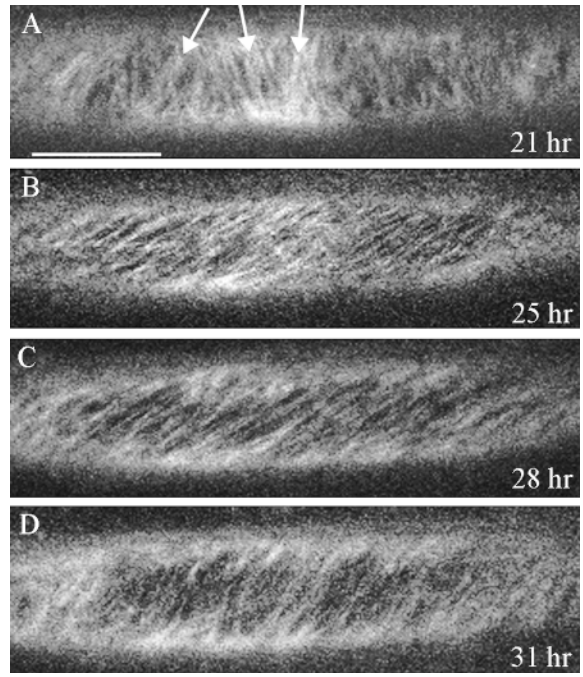

Figure 9. Time Sequence of Laser Scanning Confocal Microscopic Images of a Microtubule Array in the Cortex along the Outer Epidermal Wall of a Fava Bean Leaf Showing Net Movement in One Direction and Then in the Reverse.

A fava bean leaf was bombarded and maintained in a humid Petri dish for 21 hr and then viewed with a laser scanning confocal microscope at various times.
(A) 21 hr after bombardment.
(B) 25 hr after bombardment.
(C) 28 hr after bombardment.
(D) 31 hr after bombardment.
Most of the microtubules in the array were initially transverse or oblique with a pitch to the right or left. Thereafter, a gradual movement to the right was followed by a movement back to the left. The arrows in **(A)** point to some microtubules that appeared initially to have mixed orientations. Bar in **(A)** = 20 μm for **(A)** to **(D)**.

represent microtubules arranged in long cables, bundles, or thick crystalline aggregates. The more brightly fluorescent microtubule images appeared to branch, indicating that they were bundled. Bundling is not only a normal feature of the cortical array (Cyr and Palevitz, 1995), but it is also induced by the MBD (Olson et al., 1995). In the simplest scenario, bundling occurs when the MAP–microtubule interactions become so pervasive that the projecting and highly negatively charged C-terminal domains are charge neutralized by the bound MAPs. This freedom from charge repulsion allows such coated microtubules to interact laterally (MacRae, 1992). Interestingly, bundling seemed to be minimal in transversely oriented microtubule arrays, but it increased in oblique and, more especially, longitudinal arrays. Thus, it is likely that dimly fluorescent microtubule images represent normal, fully functional arrays (which may be somewhat bundled), whereas the highly fluorescent (and highly bundled) microtubules express an aberrant phenotype and thus are functionally impaired. Consistent with this conclusion is the finding that the thick, highly bundled, and longitudinally oriented microtubules are relatively resistant to depolymerization by antimicrotubule herbicides, compared with the dim, less bundled, and transversely oriented microtubules (data not shown). Moreover, these highly fluorescent microtubule images were very stable and changed very little in orientation over many hours or days.

Thus, we find that this construct and methodological approach offer two extraordinary possibilities for experimental studies. When expressed at low levels, GFP–MBD allows the constant monitoring of microtubule arrangements over extended periods of time, whereas at high levels, it induces an aberrant phenotype that likely inhibits normal microtubule function. Traditionally, microtubule functional analysis has relied heavily on the use of antimicrotubule herbicides. Highly expressed synthetic gene constructs, such as used here, would permit an alternative method to perturb function. It will be important to discern at what point the expression of the gene ceases merely to report the presence of microtubules and begins to alter their function. This should not be difficult because we have recently selected a suspension-cultured cell line that stably expresses the *GFP–MBD* gene; it appears to grow and divide at a rate similar to that of the wild type and possesses only dimly fluorescing microtubules (C.L. Granger, manuscript in preparation). Presumably, cells expressing high levels of the transgene could not compete (or were unable to survive) under mitotic conditions; therefore, it will likely prove necessary to use inducible promoters to perturb function, via high levels of expression, in stably transformed cell lines and plants.

GFP–MBD—Decorated Microtubules Retain Their Dynamic Character

Microtubule dynamics involve two major processes: dimer/polymer exchange, via either dynamic instability (Mitchison and Kirschner, 1984) or treadmilling (Rodionov and Borisy, 1997), and microtubule translocation, which involves movement of the microtubule polymer by molecular motors (Baas and Brown, 1997). Both of these events may contribute to microtubule reorganizations within the cortical array (Cyr and Palevitz, 1995). The GFP–MBD reporter protein allowed us to visualize microtubule dynamics of microtubules, local reorientations in small regions of the cell, and global reorganizations occurring along the entire face of the cell.

Changes in the placement of microtubules were seen (Figure 7, arrows). This microtubule appeared to grow as well as shorten, which is consistent with it being a dynamically unstable microtubule. This length change was not due to an optical sectioning artifact because we could not detect this microtubule in adjacent optical sections. Attempts at using fluorescent recovery after photobleaching (FRAP) to analyze polymer turnover proved problematic because of the high fluorescent stability of GFP. However, we were able to quantify the length change in what appears to be an individual microtubule. For example, the elongation velocity for the microtubule depicted in Figure 7 is $\sim$1 μm/min, and the shortening velocity is similar. This elongation velocity is consistent with that observed for in vitro–assembled plant microtubules at 20 μM tubulin (Moore et al., 1997), whereas the shortening velocity is considerably slower than that observed in vitro with purified tubulin. Although it is difficult to directly compare FRAP-based versus length change data, we infer that the cortical microtubules of fava bean leaf epidermal cells are less dynamic than some of those reported for Tradescantia stamen hairs (analyzed by FRAP; Hush et al., 1994). However, stamen hairs also have a relatively stable subpopulation of microtubules that remain unchanged over tens of minutes (Wasteneys et al., 1993). Leaf epidermal cells and staminal hair cells may be different in regard to polymer turnover, either because of a genuine difference in microtubule dynamics or because of a difference in the size of the stable subpopulation of microtubules. Alternatively, the microtubules may be stabilized by the MBD itself (Olson et al., 1995) or by endogenous plant MAPs. In addition to the observed length change, we also noted polymer movement. The microtubule marked with an arrow in Figure 7 appeared to move upward, which is consistent with a translocation mechanism. Hence, dynamic processes involving both polymer exchange and translocation appear to occur simultaneously.

In addition to changes in individual microtubules, reorientations also occurred in subsets of microtubules within small regions of the cell. These observations indicate that subpopulations of microtubules can respond to regional cues, independent of what is occurring in other areas of the cell. Lloyd (1994) has suggested that regional cuing may, under certain circumstances, play a seminal role in reorienting the array. How this cuing takes place is not well understood, but it could involve local changes in the physical properties of the cell wall; in fact, such local wall changes have been correlated with alterations in the organization of the cortical array (Fisher and Cyr, 1998).

The global organization of GFP-decorated microtubules, or bundles, into cylindrical arrays is similar to that seen by immunofluorescence microscopy or by microinjection in the epidermal cells of maize coleoptiles or pea stems (Zandomeni and Schopfer, 1993, 1994; Lloyd, 1994; Yuan et al., 1994, 1995; Wymer and Lloyd, 1996; Fischer and Schopfer, 1997). Microtubules along the side walls and inner and outer tangential epidermal walls are oriented transversely or at oblique angles, and they generally maintain their orientation. Microtubule alignment along the outer epidermal wall is more diverse, although it tends to be more oblique than in the internal tissues, with reorientation toward the longitudinal direction occurring during the cessation of growth (Iwata and Hogetsu, 1988, 1989).

Two general types of global reorientations were observed in this study. In some cells with low expression of the GFP–MBD protein, the cortical microtubule strands reoriented slowly back and forth within the range of the oblique angle (inclination $\pm 45°$ from the transverse plane). In the example shown in Figure 9, the microtubule strands showed a net movement from left to right within $\sim$7 hr, and then in the next 3 hr, they began moving back to the left. This back and forth movement suggests that the transverse alignment of microtubules is not absolute and static, as has previously been inferred from studies of fixed cells (Takesue and Shibaoka, 1998). We propose that a self-adjusting mechanism exists in elongating cells whereby deviation from the transverse is allowed within certain spatial limits but a net transverse orientation is maintained. We do not know how this mechanism operates; however, it is most likely of a developmental nature and may be related in some way to the deposition or physical characteristics of cellulose microfibrils (Fisher and Cyr, 1998).

The reorientation of microtubules toward the longitudinal direction may correspond to cessation of growth. A similar reorientation has been reported after microinjection of fluorescent analogs of tubulin (Yuan et al., 1994; Lloyd et al., 1996; Wymer and Lloyd, 1996) or addition of cytokinin, ethylene, abscisic acid, and a variety of other factors (Shibaoka, 1994). Reorientation can be prevented by gibberellin, auxin, or mechanical stretching (Zandomeni and Schopfer, 1993; Lloyd et al., 1996; Fischer and Schopfer, 1997). The trend toward longitudinal reorientation reported here was sometimes accompanied by extensive microtubule bundling and, ultimately, some detachment from the plasma membrane to endoplasmic locations.

Utility of the GFP–MBD Reporter Protein

Particle bombardment of the *GFP–MBD* reporter gene provides a rapid, efficient means for visualizing microtubules in vivo in a wide variety of plant species. A variety of microtubule structures, ranging from microtubules to long cables and bundles, can be seen in a variety of configurations. Moreover, their dynamics can be viewed over time within the same cell. Interestingly, at a low level of expression, microtubule orientation and dynamics appear to be normal, whereas at higher levels of expression, an aberrant phenotype appears. This offers the possibility for a unique study in which the regulation of *GFP–MBD* expression can be used to perturb the function of microtubules as well as to visualize their behavior.

METHODS

Construction of Microtubule Reporter Gene

A human codon–optimized synthetic S65T green fluorescent protein gene (*sGFP*; Chiu et al., 1996) was the generous gift of J. Sheen (Department of Molecular Biology, Massachusetts General Hospital, Boston, MA). A full-length mouse MAP4 cDNA (GenBank accession number M72414) was kindly provided by J. Olmsted (Department of Biology, University of Rochester, NY). We constructed a chimeric gene carrying *GFP* and the microtubule binding domain (MBD) of *MAP4* by using a two-step recombinant polymerase chain reaction (Higuchi, 1990). In the first step, *GFP* was amplified using Pfu DNA polymerase (with 3′ to 5′ exonuclease/proofreading activity; Stratagene, La Jolla, CA) with a forward primer containing an NcoI restriction site (*GFP* forward; 5′-ATCCATGGTGAGCAAGGGCGA-3′) and a reverse primer containing homologous sequences from the end of the GFP and the beginning of the MBD (*GFP* reverse; 5′-TTCTTC-TTGCCGGGACTTGTACAGCTCGTC-3′). Similarly, the MBD was amplified using a forward primer complementary to the *GFP* reverse primer (*MAP4* forward; 5′-GACGAGCTGTACAAGTCCCGGCAA-GAAGAA-3′) and a reverse primer containing a NotI restriction site (*MAP4* reverse; 5′-ATGCGGCCGCACCTCCTGCAGGAAA-3′). The resulting 753-bp GFP fragment (GFP nucleotide positions 3 to 744, with additional MAP4 regions and restriction site) and the 1279-bp MBD fragment (MAP4 nucleotide positions 2408 to 3661, with additional GFP regions and restriction site) were isolated from a gel.

The two fragments served as templates in a second polymerase chain reaction using only the *GFP* forward and the *MAP4* reverse primers. In this reaction, the 3′ end of the GFP fragment was annealed to the complementary 5′ end of the MBD fragment to produce a 2032-bp chimeric, in-frame-fusion gene, *GFP–MBD.* The amplified chimeric gene was isolated from a gel, digested with NcoI and NotI, and cloned into a modified pUC18 plasmid containing the cauliflower mosaic virus 35S promoter and nopaline synthase terminator (Figure 1).

Bacterial Expression of the GST–GFP–MBD Microtubule Reporter Protein and Cosedimentation with Taxol-Stabilized Microtubules

The chimeric *GFP–MBD* gene was inserted into the plasmid expression vector pGex2T (Pharmacia Biotechnology, Piscataway, NJ) containing a glutathione *S*-transferase (*GST*) gene under the control of the *lacZ* promoter. We also made a control construct lacking the MBD domain. The constructs were transformed into *Escherichia coli* BL21, and the bacteria were grown at 37°C in Luria-Bertani media (Sambrook et al.,1989) under ampicillin selection (100 μg/mL) to an OD_{600} of 0.8. To induce protein expression, we added isopentyltransgalactose (Sigma) to a 1 mM final concentration, and the bacteria

were incubated for 5 hr at 25°C. Bacteria were harvested by centrifugation (5000*g* for 10 min) and washed with PM buffer (50 mM Pipes, pH 6.9, 1 mM $MgSO_4$, and 1 mM EGTA). The washed bacteria were lysed in PM buffer containing 1 mg/mL lysozyme, 10 mM 3-([3-cholamidopropyl]dimethylammonio)-1-propanesulfonate detergent, and 25 μg/mL each phenylmethylsulfonyl fluoride, *N*-α-benzoyl-L-arginine methyl ester, and *N*-α-*p*-tosyl-L-arginine methyl ester. Bacteria were incubated in the lysis buffer at 30°C for 15 min and then briefly sonicated (15 pulses at 30% power; model 450 sonifier; Branson Ultrasonic Corp., Danbury, CT). Disrupted bacterial fragments were removed by centrifugation at 12,000*g* (for 10 min), and the supernatants containing the expressed microtubule–reporter proteins were collected. The fluorescent properties of the supernatants were analyzed with a fluorescence spectrophotometer (model LS-3; Perkin-Elmer, Oakbrook, IL). The samples were stored at −80°C before the microtubule sedimentation assays were performed.

Bovine neuronal tubulin was purified to apparent homogeneity by thermal cycling in glutamic acid followed by desalting on a Biogel P-6DG (Bio-Rad) column and by phosphocellulose chromatography (Cyr and Palevitz, 1989). Hyperstable microtubules were prepared by mixing purified tubulin with taxol (Sigma) at equimolar concentrations in PM buffer supplemented with 0.5 mM GTP and 0.5 mM $MgSO_4$. To obtain long microtubules, we added taxol to the tubulin at low concentrations (100 nM on ice); after 30 min, the assembling microtubules were then moved to room temperature. After growth (as monitored by dark-field microscopy), taxol was added to equimolar concentration to stabilize the long microtubules.

The supernatant, containing the bacterially expressed microtubule–reporter protein, was thawed on ice, supplemented with 10 μM taxol, and then clarified by centrifuging in a Beckman Airfuge (Beckman Instruments, Palo Alto, CA) at 60,000*g* for 10 min. Taxol-stabilized microtubules were then added to a final concentration of 20 μM. The mixture was incubated for 45 min at 24°C, and complexes of microtubules with bound proteins were then sedimented in a Beckman Airfuge, as before. Proteins in the supernatants and microtubule pellets were solubilized with Laemmli sample buffer (Laemmli, 1970).

Protein samples were analyzed by SDS-PAGE, according to Laemmli (1970), by using 10% resolving gels. We found that the GFP retained its fluorescence after SDS-PAGE, provided that the protein samples were not boiled before loading on the gel. After electrophoresis, the gels were placed onto a UV/blue light source (Fisher, Pittsburgh, PA) to visualize fluorescing polypeptide bands. Fluorescent images of the gel bands were recorded with a charge-coupled device camera (Hamamatsu Photonic Systems, Bridgewater, NJ) equipped with a 486- to 522-nm interference filter (Microcoatings Inc., Boston, MA).

Biolistic Transformation of Leaf Epidermal Cells and Epifluorescence Microscopy

Plasmid DNA (2.5 to 5 μg) harboring the *GFP–MBD* gene under the control of the 35S promoter was mixed with 1 mg of a 25-μL aqueous suspension of 1.0-μm gold particles (Bio-Rad). The gold–DNA suspension was dispersed with moderate vortexing and sonication in the presence of 1.25 M $CaCl_2$ and 17 mM spermidine and kept on ice for 5 to 30 min. The DNA-coated gold particles were then collected by a brief centrifugation, washed, resuspended in ethanol, and spread onto plastic carrier discs for biolistic transformation (particle delivery system-1000/He; Bio-Rad).

Plants (*Vicia faba*) were grown in soil in a controlled environment cabinet at 20 and 18°C day and night temperature, respectively. Ten-hour daylength was at a light intensity of 0.2 mmol/m^{-2}. Young leaves (4.5 to 6 cm long) were excised from 4-week-old plants and placed with their lower side up onto moist filter paper in 60-mm plastic Petri dishes. The dishes were inserted into the firing chamber, the vacuum was pumped to 25 inches Hg, and the DNA-coated gold particles were then fired into the leaves from a distance of 50 mm at a helium pressure of 1350 psi. Dishes with bombarded leaves were maintained in the dark at 24°C until microscopic examination.

For routine examination of transformation efficiency, we screened the leaves for GFP-expressing cells by using a Zeiss Axioskop microscope (Zeiss Corp., Thornwood, NJ) equipped with a 150-W xenon epifluorescent illuminator and a standard fluorescein isothiocyanate filter set (Zeiss set No. 10). We found that cells expressing high levels of GFP protein could be readily spotted in the leaves by use of an X10 plan Neofluar objective (Zeiss Corp.). For convenience, we often bombarded in the late afternoon and then began our observations the following morning. However, all reorientations reported herein were also observed at earlier times after bombardment.

Confocal Microscopy and Digital Image Analysis

Leaves with GFP-expressing cells were placed into 100-mm Petri dishes that had been fitted with a cover slip window at the bottom. To image the cells optimally, we laid the leaves in a small puddle of water and flattened them gently onto the cover slip surface. The dishes were positioned onto the inverted platform of a confocal laser scanning microscope (LSM model 410; Zeiss Corp.), and the cells were imaged using the 488-nm line of an argon laser. For image recording, we typically used an X40 plan Neofluar objective (NA 0.75; Zeiss Corp.) and a 488/543-nm dual dichroic excitation mirror with a 510- to 540-nm emission filter.

Selected cells were located at low magnification, and their X and Y positions were noted on the stage micrometer to allow subsequent relocation for time-course studies. Optical sections (six to 10) at 0.8-μm intervals were collected for each cell at each time point. The sections were obtained with the laser attenuated to the lowest power setting possible, using a 4-sec scan and four-line averaging (16 sec of total scan time). Because the cells shifted slightly between time points, we set the first optical section to the outer epidermal wall to obtain comparable stacks of optical sections throughout the experiment.

Optical sections were digitally processed and assembled using Photoshop 4.0 (Adobe Corp., Mountain View, CA). Stacks of sections from consecutive time points were aligned so that the image in the top section of one stack matched the corresponding image of the next stack. For each time point, four adjacent optical sections (each representing 0.8 μm) were combined. All images presented herein represent an extended view of the microtubule arrangements in ~3.2 μm of the cell's cortex.

ACKNOWLEDGMENTS

We thank Dr. Jen Sheen for her gift of the sGFP cDNA and Dr. Joanna Olmsted for providing a full-length MAP4 cDNA. Bean plants were generously provided by Dr. Sarah M. Assman and Joann Snyder (Department of Biology, Pennsylvania State University). We thank

Drs. Mark Guiltinan and Jill Deikman (Biotechnology Institute, Pennsylvania State University) for the use of particle delivery system-1000/He and Dr. Carol Wymer (John Innes Institute, Norwich, UK) for helpful comments. This work was supported by U.S. Department of Agriculture grants to R.J.C. (No. 98-35304-668) and T.-h.K. (No. 96-35304-3635) and an Australian Research Committee grant to J.M. (No. A19700148). The University of Sydney provided sabbatical leave support for J.M.

Received June 22, 1998; accepted August 31, 1998.

REFERENCES

Asada, T., and Shibaoka, H. (1994). Isolation of polypeptides with microtubule-translocating activity from phragmoplasts of tobacco BY-2 cells. J. Cell Sci. **107,** 2249–2257.

Baas, P.W., and Brown, A. (1997). Slow axonal transport: The polymer transport model. Trends Cell Biol. **7,** 380–384.

Baskin, T.I., and Wilson, J.E. (1997). Inhibitors of protein kinases and phosphatases alter root morphology and disorganize cortical microtubules. Plant Physiol. **113,** 493–502.

Blackman, L.M., Boevink, P., Santa Cruz, S., Palukaitis, P., and Oparka, K.J. (1998). The movement protein of cucumber mosaic virus traffics into sieve elements in minor veins of *Nicotiana clevelandii*. Plant Cell **10,** 525–537.

Blancaflor, E.B., and Hasenstein, K.H. (1995). Growth and microtubule orientation of *Zea mays* roots subjected to osmotic stress. Int. J. Plant Sci. **156,** 774–783.

Burns, R.G., and Surridge, C.D. (1994). Tubulin: Conservation and structure. In Microtubules, J.S. Hyams and C.W. Lloyd, eds (New York: Wiley-Liss), pp. 3–31.

Chalfie, M., Tu, Y., Euskirchen, G., Ward, W.W., and Prasher, D.C. (1994). Green fluorescent protein as a marker for gene expression. Science **263,** 802–805.

Chan, J., Rutten, T., and Lloyd, C. (1996). Isolation of microtubule-associated proteins from carrot cytoskeletons: A 120 kDa map decorates all four microtubule arrays and the nucleus. Plant J. **10,** 251–259.

Chiu, W.-L., Niwa, Y., Zeng, W., Hirano, T., Kobayashi, H., and Sheen, J. (1996). Engineered GFP as a vital reporter in plants. Curr. Biol. **6,** 325–330.

Christou, P. (1996). Transformation technology. Trends Plant Sci. **1,** 423–431.

Cubitt, A.B., Heim, R., Adams, S.R., Boyd, A.E., Gross, L.A., and Tsien, R.Y. (1995). Understanding, improving and using green fluorescent proteins. Trends Biochem. Sci. **20,** 448–455.

Cyr, R.J. (1991). Microtubule-associated proteins in higher plants. In The Cytoskeletal Basis of Plant Growth and Form, C.W. Lloyd, ed (San Diego, CA: Academic Press), pp. 57–67.

Cyr, R.J. (1994). Microtubules in plant morphogenesis: Role of the cortical array. Annu. Rev. Cell Biol. **10,** 153–180.

Cyr, R.J., and Palevitz, B.A. (1989). Microtubule-binding proteins from carrot. I. Initial characterization and microtubule bundling. Planta **177,** 245–260.

Cyr, R.J., and Palevitz, B.A. (1995). Organization of cortical microtubules in plant cells. Curr. Opin. Cell Biol. **7,** 65–71.

Desai, A., and Mitchison, T.J. (1997). Microtubule polymerization dynamics. Annu. Rev. Cell Dev. Biol. **13,** 83–117.

Durso, N.A., and Cyr, R.J. (1994). A calmodulin-sensitive interaction between microtubules and a higher plant homolog of elongation factor-1α. Plant Cell **6,** 893–905.

Epel, B.L., Padgett, H.S., Heinlein, M., and Beachy, R.N. (1996). Plant–virus movement protein dynamics probed with a GFP–protein fusion. Gene **173,** 75–79.

Fischer, K., and Schopfer, P. (1997). Interaction of auxin, light, and mechanical stress in orienting microtubules in relation to tropic curvature in the epidermis of maize coleoptiles. Protoplasma **196,** 108–116.

Fisher, D.D., and Cyr, R.J. (1998). Extending the microtubule/microfibril paradigm. Plant Physiol. **116,** 1043–1051.

Flanders, D.J., Rawlins, D.J., Shaw, P.J., and Lloyd, C.W. (1989). Computer-aided 3-D reconstruction of interphase microtubules in epidermal cells of *Datura stramonium* reveals principles of array assembly. Development **106,** 531–541.

Fukuda, H. (1997). Tracheary element differentiation. Plant Cell **9,** 1147–1156.

Giddings, T.H., Jr., and Staehelin, L.A. (1991). Microtubule-mediated control of microfibril deposition: A re-examination of the hypothesis. In The Cytoskeletal Basis of Plant Growth and Form, C.W. Lloyd, ed (San Diego, CA: Academic Press), pp. 85–100.

Green, P.B. (1980). Organogenesis—A biophysical view. Annu. Rev. Plant Physiol. **31,** 51–82.

Gu, X., and Verma, D.P.S. (1997). Dynamics of phragmoplastin in living cells during cell plate formation and uncoupling of cell elongation from the plane of cell division. Plant Cell **9,** 157–169.

Gunning, B.E.S., and Hardham, A.R. (1982). Microtubules. Annu. Rev. Plant Physiol. **33,** 651–698.

Haseloff, J., and Amos, B. (1995). GFP in plants. Trends Genet. **11,** 328–329.

Heim, R., and Tsien, R.Y. (1996). Engineering green fluorescent protein for improved brightness, longer wavelengths and fluorescence resonance energy transfer. Curr. Biol. **6,** 178–182.

Heinlein, M., Epel, B., Padgett, H.S., and Beachy, R. (1995). Interaction of tobamovirus movement proteins with the plant cytoskeleton. Science **270,** 1983–1985.

Hepler, P.K., and Hush, J.M. (1996). Behavior of microtubules in living plant cells. Plant Physiol. **112,** 455–461.

Higuchi, R. (1990). Recombinant PCR. In PCR Protocols, M.A. Innis, D.H. Gelfand, J.J. Sninsky, and T.J. White, eds (New York: Academic Press), pp. 177–182.

Hirokawa, N. (1994). Microtubule organization and dynamics dependent on microtubule-associated proteins. Curr. Opin. Cell Biol. **6,** 74–81.

Hugdahl, J.D., Bokros, C.L., Hanesworth, V.R., Aalund, G.R., and Morejohn, L.C. (1993). Unique functional characteristics of the polymerization and MAP binding regulatory domains of plant tubulin. Plant Cell **5,** 1063–1080.

Hush, J.M., Wadsworth, P., Callaham, D.A., and Hepler, P.K. (1994). Quantification of microtubule dynamics in living plant cells using fluorescence redistribution after photobleaching. J. Cell Sci. **107,** 775–784.

Hush, J.M., Wu, L., John, P.C.L., Hepler, L.H., and Hepler, P.K. (1996). Plant mitosis promoting factor disassembles the microtubule preprophase band and accelerates prophase progression in *Trandescantia*. Cell Biol. Int. **20,** 275–287.

Iwata, K., and Hogetsu, T. (1988). Arrangement of cortical microtubules in *Avena* coleoptiles and mesocotyls and *Pisum* epicotyls. Plant Cell Physiol. **29,** 807–815.

Iwata, K., and Hogetsu, T. (1989). The effects of light irradiation on the orientation of microtubules in seedlings of *Avena sativa* L. and *Pisum sativum* L. Plant Cell Physiol. **30,** 1011–1016.

Kropf, D.L., Williamson, R.E., and Wasteneys, G.O. (1997). Microtubule orientation and dynamics in elongating characean internodal cells following cytosolic acidification, induction of pH bands, or premature growth arrest. Protoplasma **197,** 188–198.

Laemmli, U.K. (1970). Cleavage of structural proteins during the assembly of the head of bacteriophage T4. Nature **227,** 680–685.

Liang, B.M., Dennings, A.M., Sharp, R.E., and Baskin, T.I. (1996). Consistent handedness of microtubule helical arrays in maize and Arabidopsis primary roots. Protoplasma **190,** 8–15.

Lloyd, C.W., ed (1991). The Cytoskeletal Basis of Plant Growth and Form. (San Diego, CA: Academic Press).

Lloyd, C.W. (1994). Why should stationary plant cells have such dynamic microtubules? Mol. Biol. Cell **5,** 1277–1280.

Lloyd, C.W., Shaw, P.J., Warn, R.M., and Yuan, M. (1996). Gibberellic-acid–induced reorientation of cortical microtubules in living plant cells. J. Microsc. **181,** 140–144.

Ludin, B., and Matus, A. (1998). GFP illuminates the cytoskeleton. Trends Cell Biol. **8,** 72–77.

MacRae, T.H. (1992). Microtubule organization by cross-linking and bundling proteins. Biochim. Biophys. Acta **1160,** 145–155.

Mandelkow, E., and Mandelkow, E.-M. (1995). Microtubules and microtubule-associated proteins. Curr. Opin. Cell Biol. **7,** 72–81.

Marc, J. (1997). Microtubule-organizing centres in plants. Trends Plant Sci. **2,** 223–230.

Marc, J., Mineyuki, Y., and Palevitz, B.A. (1989). The generation and consolidation of a radial array of cortical microtubules in developing guard cells of *Allium cepa* L. Planta **179,** 516–529.

Marc, J., Sharkey, D.E., Durso, N.A., Zhang, M., and Cyr, R.J. (1996). Isolation of a 90-kD microtubule-associated protein from tobacco membranes. Plant Cell **8,** 2127–2138.

McClinton, R.S., and Sung, Z.R. (1997). Organization of cortical microtubules at the plasma membrane in *Arabidopsis*. Planta **201,** 252–260.

Mitchison, T., and Kirschner, M. (1984). Dynamic instability of microtubule growth. Nature **312,** 237–242.

Mizuno, K. (1994). Inhibition of gibberellin-induced elongation, reorientation of cortical microtubules and change of isoform of tubulin in epicotyl segments of azuki bean by protein kinase inhibitors. Plant Cell Physiol. **35,** 1149–1157.

Moore, R.C., Zhang, M., Cassimeris, L., and Cyr, R.J. (1997). In vitro assembled plant microtubules exhibit a high state of dynamic instability. Cell Motil. Cytoskel. **38,** 278–286.

Morejohn, L.C. (1991). The molecular pharmacology of plant tubulin and microtubules. In The Cytoskeletal Basis of Plant Growth and Form, C.W. Lloyd, ed (San Diego, CA: Academic Press), pp. 29–44.

Nogales, E., Wolf, S.G., and Downing, K.H. (1998). Structure of the $\alpha\beta$ tubulin dimer by electron crystallography. Nature **391,** 199–203.

Olson, K.R., McIntosh, J.R., and Olmsted, J.B. (1995). Analysis of MAP4 function in living cells using green fluorescent protein (GFP) chimeras. J. Cell Biol. **130,** 636–650.

Oparka, K.J., Boevink, P., and Santa Cruz, S. (1996). Studying the movement of plant viruses using green fluorescent protein. Trends Plant Sci. **1,** 412–418.

Ormo, M., Cubitt, A.B., Kallio, K., Gross, L.A., Tsien, R.Y., and Remington, S.J. (1996). Crystal structure of the *Aequorea victoria* green fluorescent protein. Science **273,** 1392–1395.

Preuss, U., Doring, F., Illenberger, S., and Mandelkow, E.-M. (1995). Cell cycle–dependent phosphorylation and microtubule binding of tau protein stably transfected into Chinese hamster ovary cells. Mol. Biol. Cell **6,** 1397–1410.

Rizzuto, R., Brini, M., DeGiorgi, F., Rossi, R., Heim, R., Tsien, R.Y., and Pozzan, T. (1996). Double labeling of subcellular structures with organelle-targeted GFP mutants *in vivo*. Curr. Biol. **6,** 183–188.

Rodionov, V.I., and Borisy, G.G. (1997). Microtubule treadmilling *in vivo*. Science **275,** 215–218.

Sambrook, J., Fritsch, E.F., and Maniatis, T. (1989). Molecular Cloning: A Laboratory Manual. (Cold Spring Harbor, NY: Cold Spring Harbor Laboratory Press).

Sheen, J., Hwang, S., Niwa, Y., Kobayashi, H., and Galbraith, D.W. (1995). Green-fluorescent protein as a new vital marker in plant cells. Plant J. **8,** 777–784.

Shelden, E., and Wadsworth, P. (1996). Stimulation of microtubule dynamic turnover in living cells treated with okadaic acid. Cell Motil. Cytoskeleton **35,** 24–34.

Shibaoka, H. (1994). Plant hormone-induced changes in the orientation of cortical microtubules: Alterations in the cross-linking between microtubules and the plasma membrane. Annu. Rev. Plant Physiol. Plant Mol. Biol. **45,** 527–544.

Stearns, T. (1995). The green revolution. Curr. Biol. **5,** 262–264.

Takesue, K., and Shibaoka, H. (1998). The cyclic reorientation of cortical microtubules in epidermal cells of azuki bean epicotyls: The role of actin filaments in the progression of the cycle. Planta **205,** 539–546.

Traas, J., Bellini, C., Nacry, P., Kronenberger, J., Bouchez, D., and Caboche, M. (1995). Normal differentiation patterns in plants lacking microtubular preprophase bands. Nature **375,** 676–677.

van de Sande, K., Pawlowski, K., Czaja, I., Wieneke, U., Schell, J., Schmidt, J., Walden, R., Matvienko, M., Wellink, J., van Kammen, A., Franssen, H., and Bisseling, T. (1996). Modification of phytohormone response by a peptide encoded by *ENOD40* of legumes and a nonlegume. Science **273,** 370–373.

Vaughn, K.C., and Harper, J.D.I. (1998). Microtubule-organizing centers and nucleating sites in land plants. Int. Rev. Cytol. **181,** 75–149.

Vesk, P.A., Rayns, D.G., and Vesk, M. (1994). Imaging of plant microtubules with high resolution scanning electron microscopy. Protoplasma **182,** 71–74.

Wasteneys, G.O., Gunning, B.E.S., and Hepler, P.K. (1993). Microinjection of fluorescent brain tubulin reveals dynamic properties of cortical microtubules in living plant cells. Cell Motil. Cytoskeleton **24,** 205–213.

West, R.R., Tenbarge, K.M, and Olmsted, J.B. (1991). A model for microtubule-associated protein 4 structure. Domains defined by comparisons of human, mouse, and bovine sequences. J. Biol. Chem. **266,** 21886–21896.

Williamson, R.E. (1991). Orientation of cortical microtubules in interphase plant cells. Int. Rev. Cytol. **129,** 135–206.

Wymer, C.L., and Lloyd, C. (1996). Dynamic microtubules: Implications for cell wall patterns. Trends Plant Sci. **1,** 222–228.

Wymer, C.L., Fisher, D.D., Moore, R.C., and Cyr, R.J. (1996a). Elucidating the mechanism of cortical microtubule reorientation in plant cells. Cell Motil. Cytoskeleton **35,** 162–173.

Wymer, C.L., Wymer, S.A., Cosgrove, D.J., and Cyr, R.J. (1996b). Plant cell growth responds to external forces and the response requires intact microtubules. Plant Physiol. **110,** 425–430.

Yuan, M., Shaw, P.J., Warn, R.M., and Lloyd, C.W. (1994). Dynamic reorientation of cortical microtubules, from transverse to longitudinal, in living plant cells. Proc. Natl. Acad. Sci. USA **91,** 6050–6053.

Yuan, M., Warn, R.M., Shaw, P.J., and Lloyd, C.W. (1995). Dynamic microtubules under the radial and outer tangential walls of microinjected pea epidermal cells observed by computer reconstruction. Plant J. **7,** 17–23.

Zandomeni, K., and Schopfer, P. (1993). Reorientation of microtubules at the outer epidermal wall of maize coleoptiles by phytochrome, blue-light photoreceptor, and auxin. Protoplasma **173,** 103–112.

Zandomeni, K., and Schopfer, P. (1994). Mechanosensory microtubule reorientation in the epidermis of maize coleoptiles subjected to bending stress. Protoplasma **182,** 96–101.